DOI: 10.1002/ejic.201000138

Synthesis, Spectroscopic and Magnetic Properties of the $Co_2(OH)(PO_4)_{1-x}(AsO_4)_x$ $[0 \leq x \leq 1]$ Solid Solution

Imanol de Pedro,[a,b] José María Rojo,[a] Jesús Rodríguez Fernández,[b] Luis Lezama,[a] and Teófilo Rojo*[a]

Keywords: Hydrothermal synthesis / Solid solution / Spectroscopic properties / Magnetic properties / Solid-state structures / Cobalt / Arsenic

The $Co_2(OH)(PO_4)_{1-x}(AsO_4)_x$ $[0 \leq x \leq 1]$ solid solution was prepared by hydrothermal synthesis and, polycrystalline samples characterized by X-ray powder diffraction and spectroscopic measurements. The cell parameters of the isostructural phosphate–arsenate phases follow Vegard's law in the whole range of composition. The IR spectra are characteristic of three distinct features corresponding principally to the vibrations of both the hydroxide and tetrahedral $(XO_4)^{3-}$ (X = P, As) groups together with the evolution of the intensity of stretching $[\nu_{as}(X–O)]$ vibration modes corresponding to the PO_4 and AsO_4 tetrahedra in the solid solution. Diffuse reflectance data show bands belonging to the octahedral and trigonal bipyramidal geometries of the Co^{2+} ions with a high degree of covalence in the Co–O bonds of the arsenate phases. Magnetization measurements of $Co_2(OH)(PO_4)_{1-x}(AsO_4)_x$ $[0 \leq x \leq 1]$ show the existence of antiferromagnetic interactions with the presence of a ferromagnetic component below the ordering temperature. T_N decreases from 71 to 19 K as the arsenate amount is increased. ZFC-FC curves show irreversibility just below T_N for $Co_2(OH)(PO_4)_{1-x}(AsO_4)_x$ [x = 0.1–0.75]. The magnetic behavior of $Co_2(OH)(PO_4)_{0.1}(AsO_4)_{0.9}$ is completely different from the rest of the hydroxyphosphate–arsenate members and similar to that observed in the undoped arsenate compound where an incommensurate magnetic phase is observed.

Introduction

Mineral solid-state chemistry offers an important contribution to materials science in the search for systems with new and useful physical properties. The phosphate and arsenate minerals crystallize in different structures, sometimes containing several non-equivalent sites for the metals. The stoichiometries and a wide variety of structural types can make them an appropriate domain to study the relationships between the magnetic properties and the crystal packing features.[1,2] Moreover, the great ability of phosphate and arsenate frameworks to stabilize different oxidation states favors the formation of anionic constructions with a high degree of mechanical, chemical and thermal stability.[3,4]

The minerals of the olivine group, with formula $ABXO_4$, where the phosphate and arsenate anions are mainly tetrahedral ligands have been known about for a long time.[5] The adamite family, with formula $[M_2(O/OH)(XO_4)]$, belongs to this group and takes its name from the natural compound $Zn_2(OH)AsO_4$.[6,7] The mineral phases such as eveite, $Mn_2(OH)AsO_4$,[8] libethenite, $Cu_2(OH)PO_4$,[9] zincolibethenite; $(Cu,Zn)_2(OH)PO_4$[10] and synthesized compounds such as $(Mg,Ni)_2(OH)AsO_4$,[11] $Co_2(OH)PO_4$,[12] $Zn_2(OH)PO_4$[12] and $Co_2(OH)AsO_4$[13] belong to this family. In the past, the difficulty in obtaining these compounds as pure phases had hindered the study of the physical properties, but in recent years hydrothermal techniques have been successfully used to prepare them in the laboratory.[14]

The crystal structure of the $Co_2(OH)XO_4$ (X = P, As)[12,13] phases can be described as formed by two crystallographically distinct metal ions: Co(1) is fivefold coordinated by O atoms in approximately trigonal-bipyramidal geometry, with one of the apical positions occupied by OH group; Co(2) is in octaedrally distorted geometry, with two long apical Co(2)–O and four shorter equatorial bonds, two of which are hydroxide groups in *cis* configuration (see Figure 1). The structure is built up from edge-sharing strings of Co(2)–O_6 octahedra, which propagate in the *c*-direction. These Co(2) chains are cross-linked (via oxygen bridges) to pairs of edge-shared trigonal pyramidal Co(1) atoms. Finally, the anion groups [X = P, As] partake in four distinct X–O–[2 Co] bonds [each bond links to two Co(1) and/or Co(2)], resulting in a condensed structure without any identifiable channels or pores.

In recent years, many cobalt-insulator compounds have attracted much attention in solid state physics due to their interesting magnetic properties.[15] For instance, the

[a] Departamento de Química Inorgánica, Facultad de Ciencia y Tecnología, Universidad del País Vasco UPV/EHU, 48080 Bilbao, Spain
[b] CITIMAC, Facultad de Ciencias, Universidad de Cantabria, 39005 Santander, Spain

Supporting information for this article is available on the WWW under http://dx.doi.org/10.1002/ejic.201000138.

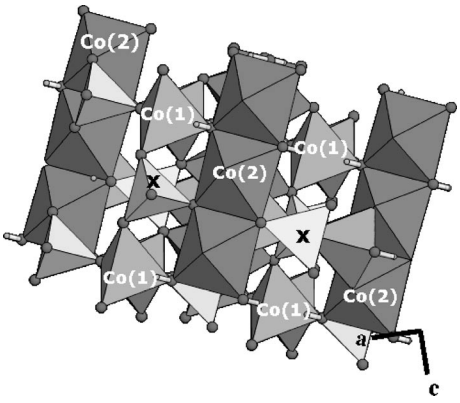

Figure 1. Schematic drawing of the $Co_2(OH)XO_4$ (X = P, As) crystal structure view along the |010| direction. Polyhedra are occupied by the Co^{II} ions and the XO_4 groups are represented by tetrahedra. Open circles correspond to the oxygen atoms, very small circles show the hydrogen atoms.

$Co_2(OH)PO_4$[16] was the first 3D antiferromagnetic ordered phosphate with a spin glass state. This behavior has been attributed to the coexistence of two ferromagnetic dimeric and chain sublattices antiferromagnetically coupled. The spontaneous static ordering of the magnetic moments at low temperatures is caused by exchange interactions between the moments with a Co(1)–O(3)–Co(2) superexchange ferromagnetic angle making it energetically favorable for them to align either parallel or antiparallel. Besides, the existence of a geometrical frustration in the Co(1) magnetic moments due to the presence of antiferromagnetic interactions between Co(2) neighbor chains and the anisotropy of the Co^{II} ions favor the spin glass-like state observed in this three-dimensional antiferromagnetic ordered phase.[16] We have recently studied the effect of the substitution of Co^{2+} (S = 3/2) by Ni^{2+} (S = 1) or Cu^{2+} (S = 1/2) ions on the nature of the magnetic anomalies at low temperatures giving rise to interesting magnetic properties in the $Co_{2-x}M_x(OH)PO_4$ (M = Ni, Cu) phases.[17,18] The substitution of the PO_4^{3-} by AsO_4^{3-} anions in the $Co_2(OH)PO_4$ phase substantially modifies the magnetic exchange Co(1)–O(3)–Co(2) angle from 107° to 116.9° for the phosphate and arsenate, respectively relaxing the magnetic frustration system of $Co_2(OH)PO_4$ and leading to an incommensurate phase with antiferromagnetic interactions (sinusoidal amplitude-modulated) in $Co_2(OH)AsO_4$.[19] In all of them the magnetic interactions propagated via |OH| and |XO_4| tetrahedra (X = P, As) give rise to a three-dimensional antiferromagnetic coupling.

The similar ability of AsO_4^{3-} and PO_4^{3-} tetrahedra to stabilize anionic frameworks and the greater size of the AsO_4^{3-} anions predict some differences in the crystal packing features that modify the complex magnetic properties exhibited in these phases. In this paper we present the synthesis, spectroscopic and magnetic properties of the $Co_2(OH)(PO_4)_{1-x}(AsO_4)_x$ [x = 0–1] solid solution in order to understand both the evolution of the magnetic properties with the substitution of the PO_4^{3-} by AsO_4^{3-} ions and the role played by the anionic groups in their complex magnetic behavior.

Results and Discussion

Crystallographic Characterization of $Co_2(OH)(PO_4)_{1-x}(AsO_4)_x$ [$0 \le x \le 1$]

The X-ray powder diffraction data were used to characterize the obtained $Co_2(OH)(PO_4)_{1-x}(AsO_4)_x$ [$0 \le x \le 1$] phases. Phosphate–arsenate cobalt(II) compounds are isostructural with $Co_2(OH)XO_4$ (X = P, As) and no extra diffraction peaks were observed in the refinements (Figure 2). All of them crystallize in the orthorhombic *Pnnm* space group. The cell parameters (see Table 1 and Figure 3) exhibit a linear variation with the phosphate substitution degree, x, following Vegard's law in the entire composition range. Rietveld refinements have been carried out and the results are given in the Supporting Information. Lattice parameters and cell volume increase with the gradual substitution of phosphate by arsenate ions. This result is in good agreement with the periodic trend in radius going down Group 15. Furthermore, the large unit cells in the arsenate compounds ($\Delta V \approx 30$ Å^3 between non-substituted phases) could modify the main bond lengths and angles in the two independent crystallographic sites for the cobalt and the tetrahedral groups corresponding to the AsO_4^{3-} groups giving rise to different exchange magnetic pathways.

Thermal Behavior

The decomposition curves of all compounds revealed weight losses in two steps[11,12] (see Supporting Information). The mean loss began above 600 °C and depended on the substitution of AsO_4 by PO_4 (see Table 1). The decomposition process was accompanied by other endothermic effects with marked peaks between 630 and 650 °C for the phosphate–arsenate compounds. The total weight loss measured during this second step (see Table 1) can be attributed to the loss of water obtained from the decomposition of two formula units of $Co_2(OH)(PO_4)_{1-x}(AsO_4)_x$ in good agreement with the thermogravimetric analysis of $M_2(OH)XO_4$ [X = P, As and M = Mg, Co] in air.[11,12] At about 700 °C additional weight losses were not observed in the thermogravimetric curves. The X-ray diffraction patterns of the residues showed the presence of CoO (PDF no. 74-1657), $Co_3(PO_4)_2$ (PDF no. 77-0225) and $Co_3(AsO_4)_2$ (PDF no. 80-2349) as final products.[20]

IR Spectroscopy

The infrared spectra for the $Co_2(OH)(PO_4)_{1-x}(AsO_4)_x$ [$0 \le x \le 1$] solid solution are represented in Figure 4. Three important sets of bands, which correspond to the vibrations of the hydroxide, phosphate and arsenate groups, can be

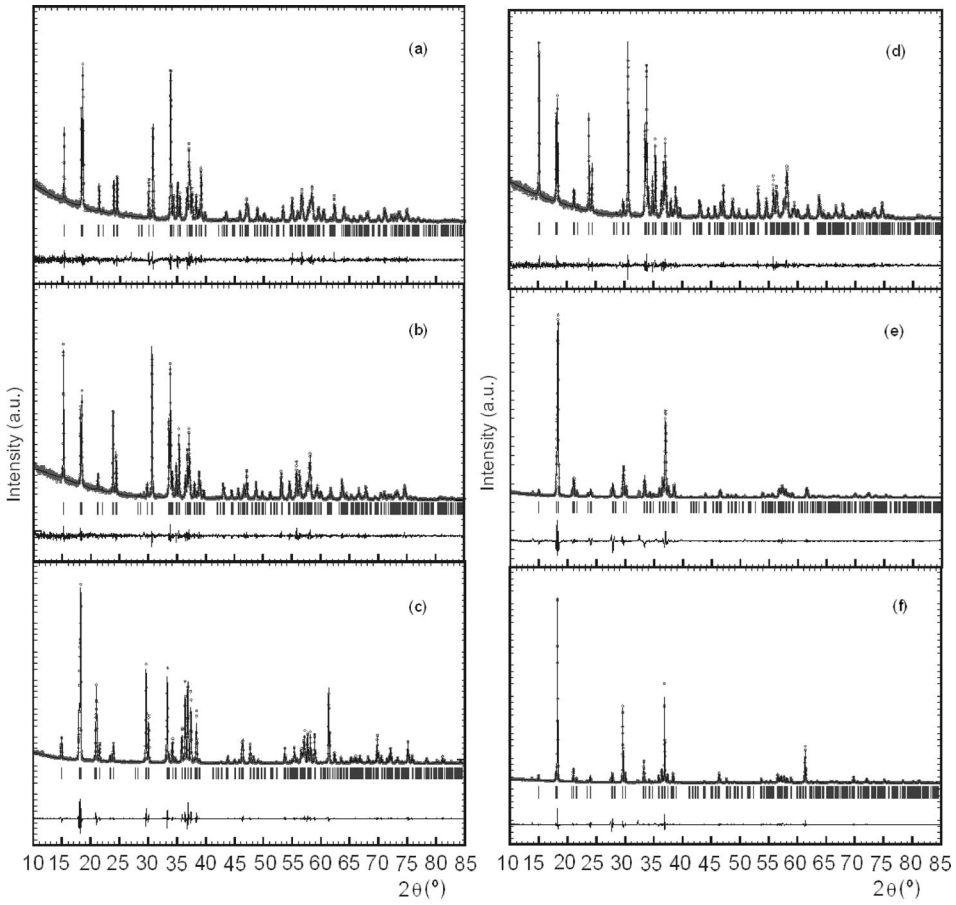

Figure 2. Observed (circles), calculated (solid line) and difference (at the bottom) X-ray powder diffraction profiles for the (a) $Co_2(OH)(PO_4)_{0.9}(AsO_4)_{0.1}$, (b) $Co_2(OH)(PO_4)_{0.75}(AsO_4)_{0.25}$, (c) $Co_2(OH)(PO_4)_{0.5}(AsO_4)_{0.5}$, (d) $Co_2(OH)(PO_4)_{0.25}(AsO_4)_{0.75}$, (e) $Co_2(OH)(PO_4)_{0.1}(AsO_4)_{0.9}$ and (f) $Co_2(OH)AsO_4$ phases at room temperature. Vertical marks correspond to the position of the allowed reflections for the crystallographic structure.

Table 1. Refined cell parameters, percentages of the elements found (and calculated) and thermogravimetric results for $Co_2(OH)(PO_4)_{1-x}(AsO_4)_x$ $[0 \leq x \leq 1]$.

	$Co_2(OH)PO_4$[a]	$Co_2(OH)(PO_4)_{0.9}(AsO_4)_{0.1}$	$Co_2(OH)(PO_4)_{0.75}(AsO_4)_{0.25}$	$Co_2(OH)(PO_4)_{0.5}(AsO_4)_{0.5}$	$Co_2(OH)(PO_4)_{0.25}(AsO_4)_{0.75}$	$Co_2(OH)(PO_4)_{0.1}(AsO_4)_{0.9}$	$Co_2(OH)AsO_4$
a [Å]	8.043(1)	8.073(1)	8.110(2)	8. 121(1)	8.213(1)	8.256(1)	8.281(1)
b [Å]	8.380(1)	8.402(2)	8.421(1)	8. 439(3)	8.514(1)	8.561(2)	8.586(1)
c [Å]	5.953(1)	5.960(2)	5.976(3)	6.010(1)	6.015(3)	6.033(1)	6.038(1)
V [Å^3]	401.3(1)	404.3(1)	409.1(1)	410.7(1)	419.2(2)	427.1(1)	429.4(1)
% Co	51.3(1)	50.0(1)	48.2(1)	46.3(1)	44.4(1)	43.1(1)	48.7(1)
% P	12.8(1)	11.7(1)	9.6(1)	6.4(1)	2.6(1)	1.3(1)	(–)
% As	(–)	3.3(1)	7.8(1)	14.7(1)	21.6(1)	24.6(1)	29.0(1)
T [°C] second step decomposition	620	640	630	680	640	650	660
% Weight loss[b]	3.6(3.8)	4.5(3.8)	5.2(3.7)	3.9(3.6)	3.8(3.4)	4.7(3.3)	3.5(3.3)
Space group *Pnnm* (No. 58), $Z = 4$							

[a] Single-crystal unit-cell parameters from $Co_2(OH)PO_4$[12]: $a = 8.042(3)$ Å, $b = 8.369(2)$ Å, $c = 5.940(2)$ Å and $V = 399.8$ Å^3 and $Co_2(OH)AsO_4$[13]: $a = 8.286(2)$ Å, $b = 8.594(2)$ Å, $c = 6.051(2)$ Å and $V = 430.9$ Å^3. [b] Experimental weight loss. The calculated values are given in parenthesis.

determined. All phases show the main features as observed in the minerals and synthetic $M_2(OH)XO_4$ (M = Mg, Zn, Co, Cu, ... and X = P, As) compounds.[7,11,21]

The presence of a sharp vibrational band at approximately 3550 cm^{-1} for all members of the solid solution (see inset Figure 4) is attributed to the stretching mode of the O–H bond and appears at a frequency similar to those observed for the isomorphous adamite and olivenite compounds.[7,22] The bands are progressively displaced from 3565 to 3540 cm^{-1} as the amount of arsenate is increased

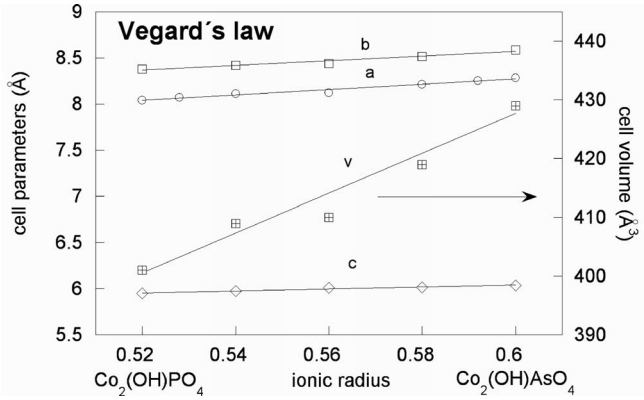

Figure 3. Evolution of the lattice parameters and cell volume for $Co_2(OH)(PO_4)_{1-x}(AsO_4)_x$ [$0 \leq x \leq 1$] from X-ray powder diffraction patterns at room temperature. The fit of variations satisfies Vegard's law.

due to the hydrogen bonding effects. Moreover, it is possible to observe another weak and broad band at 3425 cm^{-1} which could be assigned to stretching vibrations of Co–O–H groups as was shown in $Zn_2(OH)AsO_4$.[6,7] These large absorption bands together with the minor peak observed at about 1650 cm^{-1} indicate the presence of OH groups in the crystal structure and the absence of crystal-hydrate water[21b] in good agreement with the structural results.

As can be seen in Figure 4, the XO_4^{3-} (X = P, As) groups show broad and strong bands (stretch modes) between 1200–900 and 950–700 cm^{-1} corresponding to the PO_4^{3-} and AsO_4^{3-} ions, respectively. In the non-substituted phases, these bands are split in a significant way due to the presence of three different X–O distances in the XO_4 tetrahedra (see Supporting Information). The gradual substitution of the arsenate by phosphate induces the appearance of another set of bands corresponding to the stretching vibration modes of the AsO_4 groups. As expected, the relative intensity of these two sets of bands increases as the phosphate–arsenate substitution is increased.

A similar behavior is observed for the bending vibration modes of the PO_4 and AsO_4 tetrahedra. The bands appearing in the range from 650 to 500 cm^{-1} assigned to the symmetrical and asymmetrical deformation modes of the phosphate tetrahedra can be clearly observed for the $Co_2(OH)PO_4$ phase. Another set of bands appears in the 550 to 400 cm^{-1} range which is attributed to the deformation modes of the AsO_4 groups. The deformation vibrations δ(O–X–O) observed below 650 cm^{-1} are probably coupled to the corresponding antisymmetric stretching modes of the cobalt–oxygen bonds [ν_{as}(Co–O)]. These bands for the $Co_2(OH)(PO_4)_{1-x}(AsO_4)_x$ compounds, as should be expected, appear at lower frequencies when the PO_4/AsO_4 ratio decreases as corresponds to shorter X–O (X = P and As) bond lengths.[21]

In order to estimate the amount of phosphate substituted by arsenate in the $Co_2(OH)(PO_4)_{1-x}(AsO_4)_x$ [$0 \leq x \leq 1$] solid solution through IR spectroscopy, the relationship between

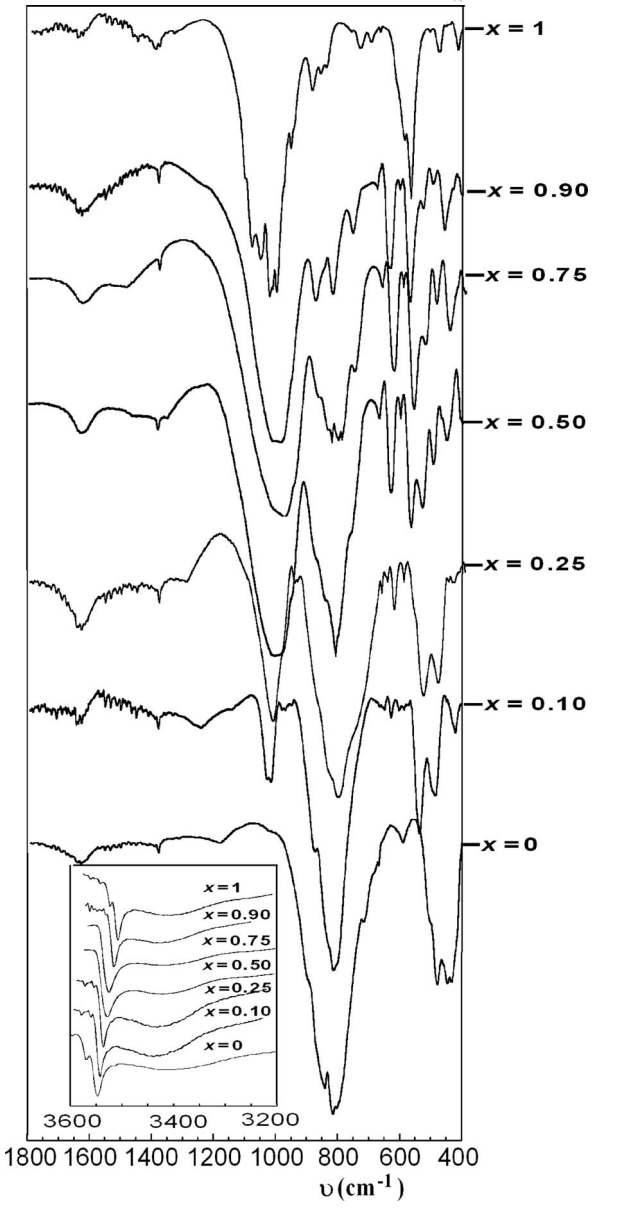

Figure 4. IR spectra of the $Co_2(OH)(PO_4)_{1-x}(AsO_4)_x$ [$0 \leq x \leq 1$] solid solution in the 1800–400 cm^{-1} region. The inset shows the 3600–3200 cm^{-1} range.

the stretching [ν_{as} (X–O)] vibration modes with the composition of the XO_4^{3-} (X = P and As) groups has been evaluated. In this way, different measurements using 1 mg of each phase and 300 mg of KBr for all preparations were carried out. The maxima intensity at the wave numbers of each phosphate and arsenate spectral bands were measured using a baseline between 1200 and 700 cm^{-1}. A linear variation was observed in all ranges of compositions, which is related to the PO_4/AsO_4 ratio (see Figure 5). In the case of $Co_2(OH)(PO_4)_{0.5}(AsO_4)_{0.5}$, the ratio is practically 50% as corresponds to bands with the same length. These results are in good agreement with those obtained from the ICP-AES and crystallographic data (see Table 1).

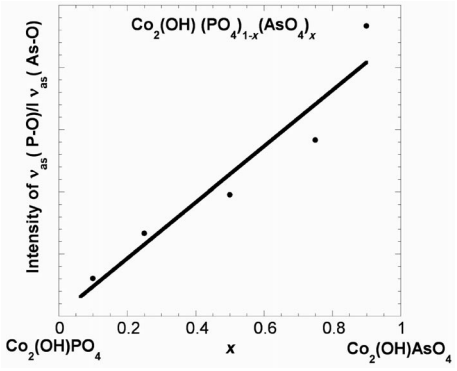

Figure 5. Relationship between the stretching vibration modes with the composition of the XO_4^{3-} (X = P and As) groups.

UV/Vis Spectroscopy

Optical data were obtained from diffuse reflectance experiments at room temperature in the 5000–50000 cm^{-1} range (see Supporting Information). The results and the assignments are given in Table 2. Using a simple crystal-field approximate model corresponding to an energy level diagram for an octahedral d^7 system, the ligand-field splitting parameter 10Dq and the Racah parameter B may be calculated from the energies of the two higher spin-allowed transitions.[23] The Dq and B Racah parameters for $Co_2OH(PO_4)_{1-x}(AsO_4)_x$ $[0.1 \leq x \leq 0.9]$ are close to those of the non-substituted compounds (see Table 2) [Dq = 720 cm^{-1} and B = 875 cm^{-1} for $Co_2(OH)PO_4$[16] and Dq = 780 cm^{-1} and B = 815 cm^{-1} for $Co_2(OH)AsO_4$,[11] respectively]. The Dq value increases as the arsenate amount is increased in the solid solution showing the ligand-field effect of the arsenate group.

Finally, the estimated Racah parameter B in $Co_2(OH)(PO_4)_{1-x}(AsO_4)_x$ $[0 \leq x \leq 1]$ solid solution is lower than the free ion (B = 971 cm^{-1}). The percentage of reduction of parameter B is about 90 and 84 for cobalt phosphate and arsenate respectively, but typical for Co^{2+} ions in distorted octahedral environments. The B parameter evolution suggests a higher degree of covalence in the Co–O bonds in the arsenate compounds due to the effect of the interatomic Co–O–X (X = P, As) distances in octahedral symmetry.

On the other hand, the trigonal bipyramid chromophore exhibits bands that can be assigned to the five spin-allowed transitions $^4A_2' \rightarrow {}^4A_1''$, $^4A_2''$, $^4E_2''$, $^4E'$, $^4E''(P)$ of the Co^{II} ions in a trigonal bipyramidal environment. All spectra show similar resolution bands to those observed in the non-substituted phases (see Table 2). The position of the bands and their assignment values are in the ranges usually found for octahedral and trigonal bipyramidal coordinated Co^{II} compounds.[16,23] Furthermore, these results are in good agreement with those obtained by Foglio et al.[24] in powder $Zn_2(OH)PO_4$ and $Mg_2(OH)AsO_4$ isomorphous phases doped with Co^{II} ions where the electron spin resonance measurements confirm the existence of two different Co^{II} chromophores.

Magnetic Properties

The thermal evolution of the molar magnetic susceptibility (field cooled-FC and zero field cooling-ZFC) for the $Co_2(OH)(PO_4)_{1-x}(AsO_4)_x$ $[0 \leq x \leq 1]$ powdered samples is shown in Figure 6 and Figure 7. The main magnetic data are summarized in Table 3. The ZFC molar susceptibility (χ_m) at 1 kOe shows two distinct behaviors depending on the amount of the substituted XO_4^{3-} (X = P, As) anion. The χ_m of the cobalt hydroxyphosphate, $Co_2(OH)PO_4$, increases from room temperature and reaches a first maximum at approximately 70 K attributed to the three-dimensional long-range order.[16] The partial substitution of PO_4^{3-} by AsO_4^{3-} anions leads to a decrease in the antiferromagnetic ordering temperature with the new T_N values of 63, 58, 45 and 40 K for 0.1, 0.25, 0.5 and 0.75 arsenate compositions, respectively (Figure 6). Furthermore, magnetization measurements of the $Co_2(OH)PO_4$ phase reveled the presence of a second maxima near to 15 K that was attributed to a spin

Table 2. Diffuse reflectance data of $Co_2(OH)(PO_4)_{1-x}(AsO_4)_x$ $[0 \leq x \leq 1]$. The non-substituted phases are included for comparison.

Co^{II}, d^7 (O_h) $^4T_{1g} \rightarrow$	$^4T_{2g}$	$^4A_{2g}$	$^4T_{1g}(P)$	B [cm^{-1}]	Dq [cm^{-1}]	% Reduction
$Co_2(OH)PO_4$ [16]	8450	15450	18350	875	720	90.1
$Co_2(OH)(PO_4)_{0.9}(AsO_4)_{0.1}$	8400	15730	18430	861	733	88.6
$Co_2(OH)(PO_4)_{0.75}(AsO_4)_{0.25}$	8360	15710	18400	842	735	86.7
$Co_2(OH)(PO_4)_{0.5}(AsO_4)_{0.5}$	8340	15740	18390	835	740	86.0
$Co_2(OH)(PO_4)_{0.25}(AsO_4)_{0.75}$	8360	15840	18380	829	748	85.4
$Co_2(OH)(PO_4)_{0.1}(AsO_4)_{0.9}$	8310	15450	18100	824	764	84.8
$Co_2(OH)AsO_4$ [11]	7700	15500	18020	815	780	83.9
Co^{II}, d^7 (BPT) $^4A'_2 \rightarrow$	$^4A''_1$, $^4A''_2$	$^4E''_2$	$^4E'$	$^4A'_2(P)$	$^4E''(P)$	
$Co_2(OH)PO_4$ [16]	6400	7000	11100	15800	19600	
$Co_2(OH)(PO_4)_{0.9}(AsO_4)_{0.1}$		6960	10900	15730	19600	
$Co_2(OH)(PO_4)_{0.75}(AsO_4)_{0.25}$		6960	10890	15710	19680	
$Co_2(OH)(PO_4)_{0.5}(AsO_4)_{0.5}$		6900	10920	15740	19710	
$Co_2(OH)(PO_4)_{0.25}(AsO_4)_{0.75}$		6940	10830	15840	19640	
$Co_2(OH)(PO_4)_{0.1}(AsO_4)_{0.9}$	6160	6920	10800	15450	19770	
$Co_2(OH)AsO_4$ [11]	5000	6250	10870	16000	19800	

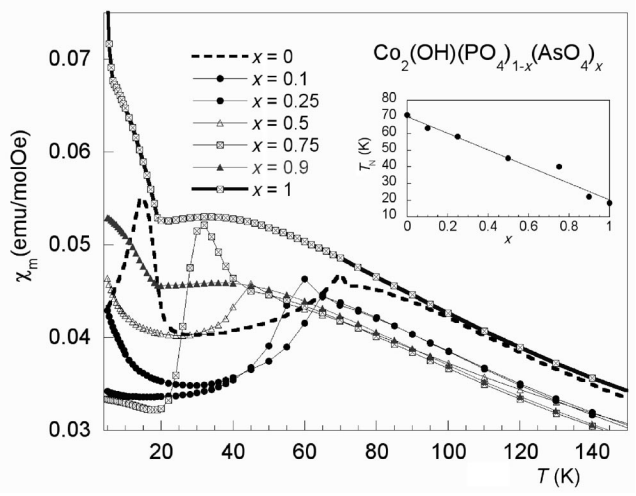

Figure 6. Thermal evolution of the molar magnetic susceptibility (zero field cooling-ZFC) at 1 kOe for $Co_2(OH)(PO_4)_{1-x}(AsO_4)_x$ [$0 \leq x \leq 1$] below 150 K. The inset shows the composition dependence of the long-range ordering temperature.

glass-like state.[16] The substitution of 10% of PO_4^{3-} by AsO_4^{3-} ions in the solid solution saw the disappearance of this maximum. However, below 20 K, an increase of the molar magnetic susceptibility in $Co_2(OH)(PO_4)_{1-x}(AsO_4)_x$ [x = 0.1–0.75] phases is observed as temperature decreases. This result could be associated to the presence of a ferromagnetic component in an overall antiferromagnetic behavior.

In the case of $Co_2(OH)(PO_4)_{0.1}(AsO_4)_{0.9}$, a similar behavior to that of the arsenate compound, $Co_2(OH)AsO_4$,[19] is observed (see Figure 6). The χ_m increases as the temperature falls below room temperature and reaches a rounded maximum at approximately 30 K that could be attributed to different origins: i) bidimensional magnetic ordering, ii) short-range magnetic interactions or iii) a crystalline electrical field.[19] Below 22 K, a strong increase in the magnetic signal is observed and this can be associated to the three-dimensional antiferromagnetic ordering as in the case of the arsenate compound.[19] However, the inflexion point located close to 6 K in the $Co_2(OH)AsO_4$ phase disappears with the

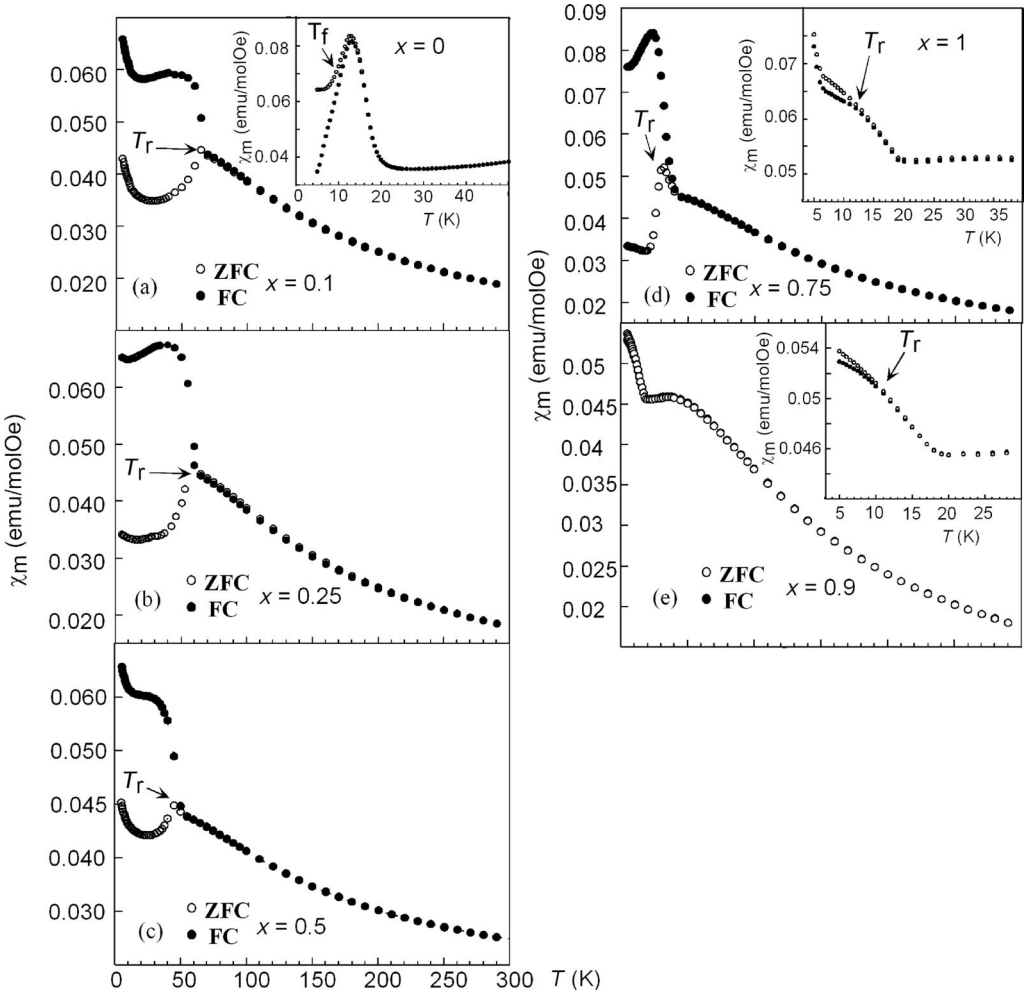

Figure 7. Low-field ZFC-FC magnetic susceptibility of (a) $Co_2(OH)(PO_4)_{0.9}(AsO_4)_{0.1}$, (b) $Co_2(OH)(PO_4)_{0.75}(AsO_4)_{0.25}$, (c) $Co_2(OH)(PO_4)_{0.5}(AsO_4)_{0.5}$, (d) $Co_2(OH)(PO_4)_{0.25}(AsO_4)_{0.75}$ and (e) $Co_2(OH)(PO_4)_{0.1}(AsO_4)_{0.9}$ phases performed at an applied field of 1 kOe. The insets show low temperature ZFC and FC measurements at 1 kOe of (a) $Co_2(OH)PO_4$, (d) $Co_2(OH)AsO_4$ and (e) $Co_2(OH)(PO_4)_{0.1}(AsO_4)_{0.9}$ phases. T_r is the temperature at which the irreversibility begins to develop.

Table 3. Selected magnetic data for the $Co_2(OH)(PO_4)_{1-x}(AsO_4)_x$ $[0 \leq x \leq 1]$ compounds. The phosphate and arsenate non-substituted cobalt compounds are included for comparison.

Compound	T_N [K]	C_m [emuK/molOe]	θ_p [K]	μ_{eff} [μB]	Reference
$Co_2(OH)PO_4$	71	3.59	– 63.5	5.36	[16]
$Co_2(OH)(PO_4)_{0.9}(AsO_4)_{0.1}$	63	3.57	–71.7	5.34	this work
$Co_2(OH)(PO_4)_{0.75}(AsO_4)_{0.25}$	58	3.47	–68.1	5.27	this work
$Co_2(OH)(PO_4)_{0.5}(AsO_4)_{0.5}$	45	3.36	–73.8	5.18	this work
$Co_2(OH)(PO_4)_{0.25}(AsO_4)_{0.75}$	40	3.35	–78.9	5.17	this work
$Co_2(OH)(PO_4)_{0.1}(AsO_4)_{0.9}$	22	3.28	–77.0	5.12	this work
$Co_2(OH)AsO_4$	19	3.26	–61.9	5.10	[19]

substitution of 10% of AsO_4^{3-} by PO_4^{3-} ions. These changes show the important effect of the anion on the magnetic behavior of these phases.

At temperatures higher than 100 K, the magnetic susceptibility data of the solid solution follow a Curie–Weiss law with Curie constants between 3.59 and 3.26 emuK/molOe and Weiss temperatures, θ_p, near –70 K (Table 3). The μ_{eff} value of the solid solution decreases from 5.36 to 5.10 μ_B; which is consistent with the literature report for high spin d^7 Co^{II} ion.[25] The negative temperature intercepted together with the decrease of the effective magnetic moment observed when the temperature is lowered are in good agreement with the predominance of antiferromagnetic interactions between neighboring Co^{II} ions in these compounds.[16,19]

The ZFC-FC curves at 0.1 T are given in Figure 7. For the $Co_2(OH)(PO_4)_{1-x}(AsO_4)_x$ $[0.1 \leq x \leq 0.75]$ samples, a paramagnetic behavior without any difference between ZFC and FC magnetization is observed at temperatures above T_N. In contrast, a significant irreversibility begins to develop at $T = T_r$ it being close to T_N. These results are quite different from those shown for the non-substituted phosphate phase[16] [see inset Figure 7 (a)] in which the irreversibility only appears below its freezing temperature, T_f. Moreover, the lack of ZFC-FC reversibility of the $Co_2(OH)(PO_4)_{1-x}(AsO_4)_x$ $[0.1 \leq x \leq 0.75]$ phases is also a characteristic of the magnetic behavior of other bimetallic phosphates such as $(Co,M)_2(OH)PO_4$ (M = Ni, Cu),[17,18] which was attributed to the presence of ions with different spin [Co^{II} (S = 3/2); Ni^{II} (S = 1) and Cu^{II} (S = 1/2)].

The magnetic behavior of the $Co_2(OH)(PO_4)_{1-x}(AsO_4)_x$ (x = 0.9, 1) phases presents significant differences in the thermal evolution of the molar magnetic susceptibility with respect to the other members of the solid solution [see insets in Figure 7 (d) and (e)] under a magnetic field of 0.1 T. The FC curve in both compounds is practically reversible and follows the same pathway independently of how the temperature is approached. At temperatures higher than 12 K no differences between zero field cooled and field cooled magnetization were observed. Below this temperature, the ZFC-FC curves show a small splitting characteristic of ferromagnetic interactions as was shown in the non-substituted cobalt-arsenate phase in which saturation is not reached even up to 90 kOe.[19] Finally, the disappearance of the inflexion point close to 6 K observed in $Co_2(OH)AsO_4$ with a slight amount of PO_4 substitution (10%) reveals changes in the magnetic ordering that could be associated with variations in the magnetic pathways of the incommensurate magnetic structure of the $Co_2(OH)AsO_4$ phase.[19]

The thermoremanent magnetization (TRM) of the $Co_2(OH)(PO_4)_{1-x}(AsO_4)_x$ solid solution, as a function of temperature is given in Figure 8. The remanent magnetization (Mr) curves were measured at H = 0 after cooling from $T > T_N$ to 4.2 K with a magnetic field of 0.1 T. The TRM curves depend on the PO_4/AsO_4 ratio, showing a direct relationship with the temperature in which the paramagnetic state is reached (Mr = 0 emu/mol). The remanent magnetization values for $Co_2(OH)PO_4$ decreases as the temperature increases up to 7 K where an up-turn is observed.[16] After a small maximum at T = 13 K (Mr ≈ 34 emu/mol) the TRM strongly decreases and then, between 20 and 50 K, the remanent magnetization stays practically constant with a value of 5 emu/mol. By increasing the temperature to higher than 70 K, the remanent magnetization falls to zero, as corresponds to a paramagnetic state. The partial substitution of PO_4^{3-} by AsO_4^{3-} anions leads to a decrease in the paramagnetic state down to 63, 58 and 45 K for x = 0.1, 0.25 and 0.5 arsenate compositions, respectively. In these compounds the TRM starts to increase below T_N and then remains almost constant down to 4.2 K. This behavior shows that the intensity of the ferromagnetic component is virtually independent of the temperature. The $Co_2(OH)(PO_4)_{0.25}(AsO_4)_{0.75}$ phase initially presents a similar behavior to that observed in the $Co_2(OH)(PO_4)_{1-x}(AsO_4)_x$ (x = 0.1, 0.25 and 0.5) phases exhibiting a maximum at 24 K (Mr ≈ 35 emu/mol). However, from this temperature to 4 K the TRM presents a continuous drop in the Mr values without a region of constant remanent magnetization. In the $Co_2(OH)(PO_4)_{0.1}(AsO_4)_{0.9}$ phase (see inset in Figure 8), surprisingly, the remanent magnetization is very weak (Mr ≈ 1 emu/mol) taking into account that the maximum remanent magnetization of $Co_2(OH)(PO_4)_{0.25}(AsO_4)_{0.75}$ is twice as intense as that observed in the other phosphate–arsenates of the solid solution. Finally, as was expected, $Co_2(OH)AsO_4$ presents a similar TRM behavior to that observed in $Co_2(OH)(PO_4)_{0.1}(AsO_4)_{0.9}$. Both compounds show a continuous decrease of the remanent magnetization with increasing temperature up to 6 K [from 1.2 and 4 to 0.5 and 2 emu/mol for $Co_2(OH)(PO_4)_{0.1}(AsO_4)_{0.9}$ and $Co_2(OH)AsO_4$, respectively]. At about 10 K a new decrease in the remanent magnetization is observed reaching the paramagnetic state at approximately 12 K.

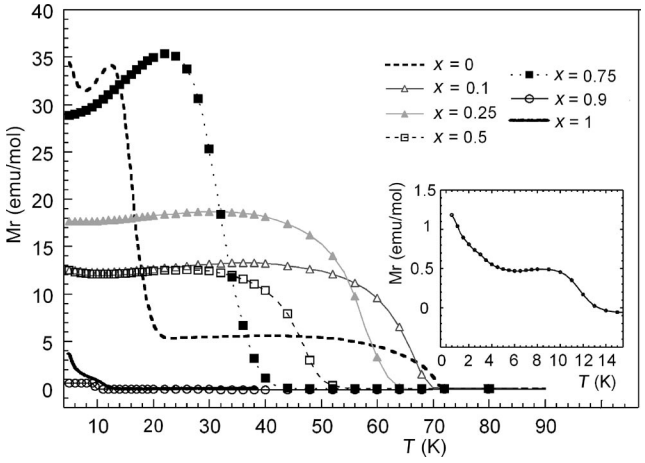

Figure 8. Temperature dependence of the thermoremanent magnetization (TRM) for $Co_2(OH)(PO_4)_{1-x}(AsO_4)_x$ $[0 \leq x \leq 1]$. The inset shows an enlargement of the TRM curve of $Co_2(OH)(PO_4)_{0.1}(AsO_4)_{0.9}$.

The existence of a remanent magnetization different from 0 below T_N in the $Co_2(OH)(PO_4)_{1-x}(AsO_4)_x$ (x = 0.1, 0.25, 0.5 and 0.75) reflects the existence of a ferromagnetic component. In fact, the magnetization variation with the magnetic field at T = 5 K shows a small hysteresis loop in which the *Hc* and *Mr* values are lower that 50 Oe and 30 emu/mol, respectively (see Figure 9). At this temperature saturation is not reached, as was observed in $(Co,M)_2(OH)PO_4$ (M = Mn, Ni and Cu).[16–18,26] Therefore, the weak ferromagnetic coupling shown in $Co_2(OH)PO_4$[16] remains until there is a 75% substitution of arsenate, developing into a magnetization in different stages for higher arsenate concentration, as was observed in the $Co_2(OH)AsO_4$ phase.[19]

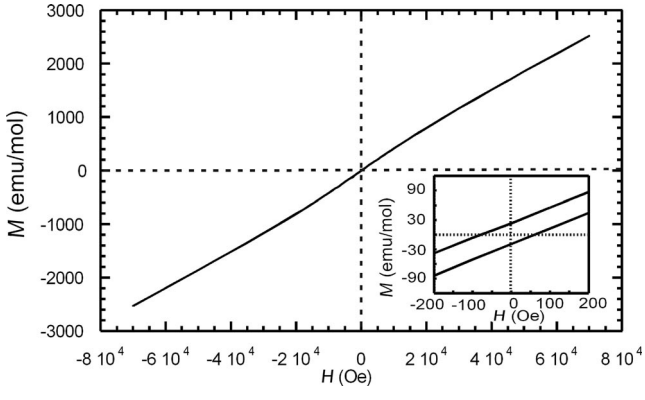

Figure 9. Magnetization vs. applied magnetic field at 5 K of $Co_2(OH)(PO_4)_{0.25}(AsO_4)_{0.75}$ phase. The inset shows an enhancement of the low-field region.

In summary, the magnetic behavior of the $Co_2(OH)(PO_4)_{1-x}(AsO_4)_x$ $[0 \leq x \leq 1]$ phases shows a magnetic evolution from a three-dimensional antiferromagnetic system with a spin glass state, $Co_2(OH)PO_4$, to an incommensurate antiferromagnetic ordering at lower temperature, in $Co_2(OH)AsO_4$ phase. In order to understand the change of the magnetic behavior as the amount of AsO_4^{3-} ions is increased, neutron diffraction measurements are necessary. Preliminary results show that the antiferromagnetic commensurate structure observed in the $Co_2(OH)PO_4$ phase remains stable up to x = 0.75 substitution, changing into an incommensurate antiferromagnetic structure along the *b* direction for higher arsenate substitutions.

Conclusions

A solid solution, $Co_2(OH)(PO_4)_{1-x}(AsO_4)_x$ $[0 \leq x \leq 1]$, with adamite-type structure has been synthesized under hydrothermal conditions. Rietveld analysis suggests an evolution of the unit cell parameters following Vegard's law in the entire composition range. The IR spectra show the evolution of the bands corresponding to the PO_4 and AsO_4 tetrahedra, making it possible to obtain the amount of them in each phase following the intensity of the stretching vibration modes [ν(X–O)] from the XO_4 groups. Spectroscopy study by diffuse reflectance reveals the existence of bands which can be adscribed to the two coordination polyhedra, octahedral and trigonal bipyramidal. In the case of the octahedral environments, the values of the *Dq* and *B* parameters are characteristic of Co^{II} ions showing a significant degree of covalence in the cobalt–oxygen bonds. The hydroxyphosphate–arsenate cobalt(II) phases exhibit a complex magnetic behavior with a 3D antiferromagnetic ordering and magnetic anomalies at low temperatures. The spin glass-like state observed in $Co_2(OH)PO_4$ at low temperatures disappears as the introduction of AsO_4 groups is increased. The substitution of PO_4^{3-} by AsO_4^{3-} ions decreases the magnetic ordering temperature, there appearing a magnetic irreversibility at approximately the Neel temperature. However, in the $Co_2(OH)(PO_4)_{0.9}(AsO_4)_{0.1}$ phase, a small irreversibility appears at about 10 K, which is lower than the Neel temperature (T_N = 22 K), showing similar behavior to that observed in $Co_2(OH)AsO_4$, where an incommensurate phase appears below 20 K. The existence of remanent magnetization below the ordering temperature up to 75% substitution of PO_4 by AsO_4 reflects the presence of ferromagnetic interactions in these compounds giving rise to magnetization in different stages in the $Co_2(OH)AsO_4$ phase.

Experimental Section

Synthesis and Structural Characterization: The $Co_2(OH)(PO_4)_{1-x}(AsO_4)_x$ $[0 \leq x \leq 1]$ compounds were prepared by hydrothermal synthesis. The $Co_3(XO_4)_2{\cdot}8H_2O$ (X = P, As) precursors were synthesized by adding dilute solutions of H_3PO_4 and As_2O_5 with $CoCl_2{\cdot}nH_2O$ following a method previously described.[27,28] Due to the low solubility of the Co^{II}-hydrated arsenates, solutions with pH values in the 6–8 range and long reaction times were needed to obtain the precipitates. A mixture of stoichiometric amounts of $Co_3(XO_4)_2{\cdot}8H_2O$ (X = P, As) was used as the starting compounds. Approximately 0.2 g of these precursors were disgregated in 35 mL of water and placed in a poly(tetrafluoroethylene)-lined stainless steel container under autogenous pressure generated by a temperature of about 170 °C for one week. Microcrystalline purple powdered samples were obtained and recovered by filtration, washed with distilled water and ethanol and dried with P_2O_5 for 24 h. The content of the Co, P and As was determined by inductively coupled

plasma atomic emission spectroscopy (ICP-AES) performed with an ARL Fisons 3410 spectrometer. The results are given in Table 1 and are consistent with the stoichiometries of: $Co_2(OH)(PO_4)_{0.9}(AsO_4)_{0.1}$; $Co_2(OH)(PO_4)_{0.75}(AsO_4)_{0.25}$; $Co_2(OH)(PO_4)_{0.5}(AsO_4)_{0.5}$; $Co_2(OH)(PO_4)_{0.25}(AsO_4)_{0.75}$ and $Co_2(OH)(PO_4)_{0.1}(AsO_4)_{0.9}$.

The X-ray powder diffraction data were used to evaluate the purity of the phosphate–arsenate products obtained in the synthesis. The powder diffraction patterns of $Co_2(OH)(PO_4)_{1-x}(AsO_4)_x$ [x = 0–1] were recorded on a Philips X′Pert-MPD x-ray diffractometer in Bragg–Brentano geometry, using graphite-monocromated Cu-K_α radiation. The data collection took place in the 10–90° 2θ, every 0.02°, with 16 seconds per step. The data were fitted using the pattern matching routine of the program FULLPROF,[29] in orthorhombic cells with the *Pnnm* space group, as previously determined from single crystal data by Harrison et al.[12] and Riffel et al.[13] for the $Co_2(OH)PO_4$ and $Co_2(OH)AsO_4$ phases, respectively. The X-ray refined unit-cell parameters are shown in Table 1. The experimental, calculated and difference XRD patterns of the $Co_2(OH)(PO_4)_{1-x}(AsO_4)_x$ [x = 0–1] polycrystalline samples are shown in Figure 2.

Physicochemical Characterization Techniques: The thermogravimetric (TGA) and differential thermal analyses (DTA) of $Co_2(OH)(PO_4)_{1-x}(AsO_4)_x$ [x = 0–1] were performed on a computer-controlled Perkin–Elmer TGA-DSC System 7 thermobalance. 100 mg of each sample were heated in air with a heating rate of 5 °C min^{-1} from 25 to 800 °C.

Spectroscopic measurements of $Co_2(OH)(PO_4)_{1-x}(AsO_4)_x$ [$0 \leq x \leq 1$] were studied by both infrared and diffuse reflectance data. The IR spectra (KBr pellets) were obtained with a MATTSON 1000 FT-IT spectrometer in the 400–4000 cm^{-1} range. The absorbance spectra of the polycrystalline samples were registered at room temperature by diffuse reflectance technique on a Cary 2415 UV/Vis-IR spectrometer in the 5000–50000 cm^{-1} range.

Magnetic susceptibility measurements (dc) of polycrystalline samples were performed using a Quantum Design MPMS-7 SQUID magnetometer whilst heating from 2 K to 300 K in an applied magnetic field of 0.1 T, after cooling either in the presence (field cooling-FC) or absence (zero field cooling-ZFC) of the applied field. Magnetization as a function of field (H) was measured using the same MPMS-7 SQUID magnetometer in the range $-7 \leq H/T \leq 7$ at a temperature range of 5–100 K after cooling the sample in zero field.

Supporting Information (see also the footnote on the first page of this article): Thermogravimetric and absorbance spectra, X-ray and IR data.

Acknowledgments

This work was financially supported by the Universidad del País Vasco/EHU UPV/EHU GIU06/11 and by Ministerio de Educación y Ciencia (MEC) (research projects MAT 2007-66737-c02-01 and MAT 2008-06542-c04).

[1] D. E. C. Corbridge, *The Structural Chemistry of Phosphorus*, Elsevier, Amsterdam, **1974**.
[2] T. Kanazawa, *Inorganic Phosphate Materials*, Elsevier Science Publishers, Amsterdam, **1989**.
[3] R. C. Haushalter, L. A. Mundi, *Chem. Mater.* **1992**, *4*, 31–48.
[4] A. Clearfield, *Chem. Rev.* **1988**, *88*, 125–148.
[5] W. E. Richmond, *Am. Mineral.* **1940**, *25*, 441–479.
[6] F. C. Hawthorne, *Can. Mineral.* **1976**, *14*, 143–148.
[7] R. J. Hill, *Am. Mineral.* **1976**, *61*, 979–986.
[8] P. B. Moore, *Ark. Mineral. Geol. Band.* **1968**, *26*, 473–476.
[9] A. Cordsen, *A Mineral.* **1978**, *16*, 153–157; P. Séller, H. Hess, F. Zettler, *Neues Jahrb. Mineral., Abh.* **1979**, *334*, 27–34.
[10] R. S. W. Braithwaite, R. G. Prichard, W. H. Paar, R. A. D. Pattrick, *Mineral. Mag.* **2005**, *69*, 145–153.
[11] J. M. Rojo, J. L. Mesa, J. L. Pizarro, L. Lezama, M. I. Arriortua, T. Rojo, *J. Solid State Chem.* **1997**, *132*, 107–112.
[12] W. T. A. Harrison, J. T. Vaughey, L. L. Dussack, A. J. Jacobson, T. E. Martin, G. D. Stucky, *J. Solid State Chem.* **1995**, *114*, 151–158.
[13] H. Riffel, F. Zettler, H. Hess, *Neues. Jahrb. Mineral. Monatsh.* **1975**, 514–517.
[14] J. M. Rojo, Ph. D. Thesis, Universidad del País Vasco, Bilbao, **2000**.
[15] a) S. Agrestini, L. C. Chapon, A. Daoud-Aladine, J. Schefer, A. Gukasov, C. Mazzoli, M. R. Lees, O. A. Petrenko, *Phys. Rev. Lett.* **2008**, *101*, 097207/1–097207/4; b) R. D. Adams, R. Layland, C. Payen, T. Datta, *Inorg. Chem.* **1996**, *35*, 3492–3494; c) S. Kobayashi, S. Mitsuda, M. Ishikawa, K. Miyatani, K. Kohn, *Phys. Rev. B* **1999**, *60*, 3331–3345; d) Z. He, J. I. Yamaura, Y. Ueda, W. Cheng, *J. Am. Chem. Soc.* **2009**, *131*, 7554–7555; e) Z. He, D. Fu, T. Kyömen, T. Taniyama, M. Itoh, *Chem. Mater.* **2005**, *17*, 2924–2929 and; f) Z. He, D. Fu, T. Kyömen, T. Taniyama, M. Itoh, *Phys. Rev. B* **2005**, *72*, 172403/1–172403/4.
[16] J. M. Rojo, J. L. Mesa, L. Lezama, J. L. Pizarro, M. I. Arriortua, J. Rodríguez Fernández, G. E. Barberis, T. Rojo, *Phys. Rev. B* **2002**, *66*, 094406/1–094406/13.
[17] I. de Pedro, J. M. Rojo, J. L. Pizarro, J. Rodríguez Fernández, J. Sánchez-Marcos, M. I. Arriortua, T. Rojo, *J. Phys.: Condens. Matter* **2006**, *18*, 3767–3787.
[18] I. de Pedro, J. M. Rojo, J. M. Pizarro, J. Rodríguez Fernández, J. Sánchez-Marcos, M. T. Fernández-Díaz, M. I. Arriortua, T. Rojo, *J. Mater. Chem.* **2007**, *17*, 3915–3926.
[19] I. de Pedro, J. M. Rojo, J. Rodríguez Fernández, M. T. Fernández-Díaz, T. Rojo, *Phys. Rev. B* **2010**, *81*, 134431/1–134431/14.
[20] *Powder Diffraction File-Inorganic and Organic*, ICDD, Pennsylvania, PA, **1995**.
[21] a) I. de Pedro, J. M. Rojo, M. Insausti, J. L. Mesa, M. I. Arriortua, T. Rojo, *Z. Anorg. Allg. Chem.* **2005**, *631*, 2096–2100; b) R. S. W. Braithwaite, *Mineral. Mag.* **1983**, *47*, 51–57; c) K. Nakamoto, *Infrared and Raman Spectra of Inorganic and Coordination Compounds*, 5th ed., John Wiley & Sons, New York, **1997**; d) I. de Pedro, J. M. Rojo, V. Jubera, J. Rodríguez Fernández, J. Sánchez-Marcos, L. Lezama, T. Rojo, *J. Mater. Chem.* **2004**, *14*, 1157–1163.
[22] P. Keller, *Neues Jahrb. Mineral. Monatsh.* **1971**, 560–564.
[23] A. B. P. Lever, *Inorganic Electronic Spectroscopy*, Elsevier *Science* Amsterdam, **1984**.
[24] M. E. Foglio, M. C. dos Santos, G. E. Barberis, J. M. Rojo, J. L. Mesa, L. Lezama, T. Rojo, *J. Phys.: Condens. Matter* **2002**, *14*, 2025–2041.
[25] a) K. L. Zhanga, Z. Wangb, H. Huangb, Y. Zhuc, X. Z. You, *J. Mol. Struct.* **2004**, *693*, 193–197; b) R. L. Carlin, *Magnetochemistry*, Springer, Berlin, Heidelberg, **1986**.
[26] I. de Pedro, J. M. Rojo, L. Lezama, T. Rojo, *Z. Anorg. Allg. Chem.* **2007**, *633*, 1847–1852.
[27] T. Rojo, L. Lezama, J. M. Rojo, M. Insausti, M. I. Arriortua, G. Villeneuve, *Eur. J. Solid State Inorg. Chem.* **1992**, *29*, 217–228.
[28] J. M. Rojo, J. L. Mesa, J. L. Pizarro, L. Lezama, M. I. Arriortua, T. Rojo, *Mater. Res. Bull.* **1996**, *31*, 925–934.
[29] J. Rodríguez-Carvajal, "FULLPROF Program for Rietveld Refinement and Pattern Matching Analysis of Powder Patterns", *Physica B* **1993**, *192*, 55, and unpublished later versions. The program is a strongly modified version of that described by D. B. Wiles, R. A. Young, *J. Appl. Crystallogr.* **1981**, *14*, 149.

Received: February 5, 2010
Published Online: May 7, 2010

